Norwegian-Type and Cold Front Aloft–Type Cyclones East of the Rocky Mountains

JOHN D. LOCATELLI, RALPH D. SCHWARTZ, MARK T. STOELINGA, AND PETER V. HOBBS

Department of Atmospheric Sciences, University of Washington, Seattle, Washington

(Manuscript received 23 March 2001, in final form 2 October 2001)

ABSTRACT

Conventional data and mesoscale model simulations are used to analyze two cyclones that developed east of the Rocky Mountains in June and November 1998. Both cyclones formed when a Pacific cold front overtook a lee trough/dryline east of the Rockies. In one case the leading edge of the Pacific cold front was on the surface, as depicted in the classic Norwegian model of a cyclone. In the other case, which is referred to as a cold front aloft (CFA) cyclone, the leading edge of the Pacific cold front was aloft and in advance of the lee trough. The lifting and severe weather associated with the Pacific cold front was along the leading edge of this front in both the Norwegian-type and CFA-type cyclones.

To obtain an estimate of how often CFA cyclones, with a coincident CFA rainband, occurred in the central United States during the period 15 September 1994 through 15 September 1995, 70 cyclones that maintained closed surface low pressure centers for at least 24 h, and produced precipitation in the United States east of the Rockies, were analyzed. Analysis of these cyclones revealed that 46% were CFA type, 23% were Norwegian type, and the remaining 31% could not be readily classified into either type. Lee troughs were common features east of the Rocky Mountains during this period. They were present in 62% of the 70 cyclones analyzed.

The 1000–500-hPa thickness field is suggested as a useful tool in locating the leading edge of a Pacific cold front, and in determining whether a cyclone is a Norwegian type or CFA type. The issue of how the frontal structures in CFA-type cyclones should be analyzed on surface weather charts is discussed, and some suggestions offered.

1. Introduction

The Norwegian conceptual model for the structure and evolution of cyclones in midlatitudes (Bjerknes and Solberg 1922) has been used for decades in the analysis of weather systems over the United States, even though its formulation was based on studies of marine cyclones approaching northwestern Europe. Its limitations are now well known. For example, it does not account for the formation of organized precipitation systems in the warm sector (e.g., Harrold 1973; Browning and Monk 1982). The limitations of the Norwegian model are significant in the central United States, due to the unique geography and airflow patterns of this region. Several investigators have described weather phenomena that are affected by the geography of the central United States, and therefore are not included in the classical Norwegian model. Surface features include lee troughs (Carlson 1961; Steenburgh and Mass 1994) and drylines (Fujita 1958; McGuire 1962; Schaefer 1974, 1986). Other investigators (Holzman 1936; Lichtblau 1936; Lloyd 1942; Williams 1953; Hobbs et al. 1990) have documented cold fronts aloft (CFA) and have associated them with precipitation and severe weather. That is not to say that the Norwegian model is not a good description of many storms that occur in the Midwest. In fact, this study will conclude that many cyclones in the central United States are well described by the Norwegian model. However, this study will also show that a significant fraction of cyclones in this region contain CFAs, a feature that forecasters should be aware of because a CFA can trigger severe weather along its length; furthermore, this study is intended to aid forecasters by showing a comparison between two severe-weather-producing cyclones, one a classical Norwegian type, and the other a cyclone containing a CFA.

Many of the nonclassical weather features that occur in the central United States are incorporated in a conceptual model for cyclones, the Structurally Transformed by Orography Model (STORM), introduced by Hobbs et al. (1996). The STORM conceptual model contains several surface features, including the lee trough/dryline (or drytrough) and the arctic front. However, the most important element of the STORM conceptual model is the CFA rainband, which can be associated with severe weather from the Rocky Mountains to the east coast (Businger et al. 1991; Locatelli et al. 1998; Neiman et al. 1998; Neiman and Wakimoto 1999; Stoelinga et al. 2000). Therefore, in this paper, to focus

Corresponding author address: Peter V. Hobbs, Department of Atmospheric Sciences, University of Washington, Box 351640, Seattle, WA 98195-1640.
E-mail: phobbs@atmos.washington.edu

attention on the CFA aspect of cyclones (and to avoid possible confusion between the acronym STORM and the common noun storm), we will use the term CFA-type (rather than STORM-type) to refer to cyclones that contain a CFA and a CFA rainband, regardless of whether or not other features of the STORM conceptual model are present.

The main goal of this paper is to use conventional and mesoscale model analysis to describe the differences between the two sample cyclones that developed east of the Rocky Mountains in June and November of 1998. Both cyclones contained rainbands over 1800 km long that were produced by lifting along a Pacific cold front, and both rainbands produced severe weather. The November 1998 cyclone was associated with multiple tornadoes and thunderstorms, and winds greater than 50 kt; the June 1998 cyclone produced winds over 68 kt, 7-cm-diameter hail, widespread flooding, downed trees and power lines, and flash floods. The 18–19 June 1998 cyclone closely fits the CFA-type cyclone model, while the 9–10 November 1998 cyclone fits the Norwegian-type cyclone model.

A secondary goal of this paper is to determine the importance of CFA-type cyclones in the forecasting of precipitation in the central United States. To address this goal, we analyzed all of the cyclones for the period 15 September 1994 through 15 September 1995 that maintained closed surface low pressure centers for at least 24 h and produced precipitation in the United States east of the Rockies. There were 70 such cyclones. We determined how many of these cyclones contained rainbands that were coincident with a CFA (i.e., CFA-type cyclones), and how many contained rainbands that were coincident with surface cold fronts that are tipped back in the vertical (Norwegian-type cyclones). While not statistically significant, this study indicates the importance of the CFA concept in forecasting.

2. The two cyclones

We will compare the two cyclones at three stages in their lifetimes: initial, developing, and mature. The *initial stage* represents the time period from when the low pressure center developed in the lee of the Rocky Mountain but before the Pacific cold front has overtaken the lee trough. The *developing stage* is the period during which the Pacific cold front overtakes the lee trough. The *mature stage* occurs when the Pacific cold front of the cyclone has reached the Mississippi River basin and the structure of the cyclone is fully formed. Since the two cyclones developed at different rates, the time periods for these three stages differ for the two cyclones.

a. Initial stage

Figure 1a shows a surface analysis for the Norwegian-type cyclone at 1800 UTC 9 November 1998, and Fig. 1b shows a surface analysis for the CFA-type cyclone at 0000 UTC 18 June 1998. These surface maps show that during their initial stages of development the cyclones were remarkably similar in their sea level pressure and surface frontal structures. Both cyclones had a low pressure center of about 997 hPa in western Kansas, an inverted trough north of the low center, a lee trough/dryline south of the low center, and an approaching Pacific cold front extending from the low pressure centers southwestward through New Mexico. The CFA-

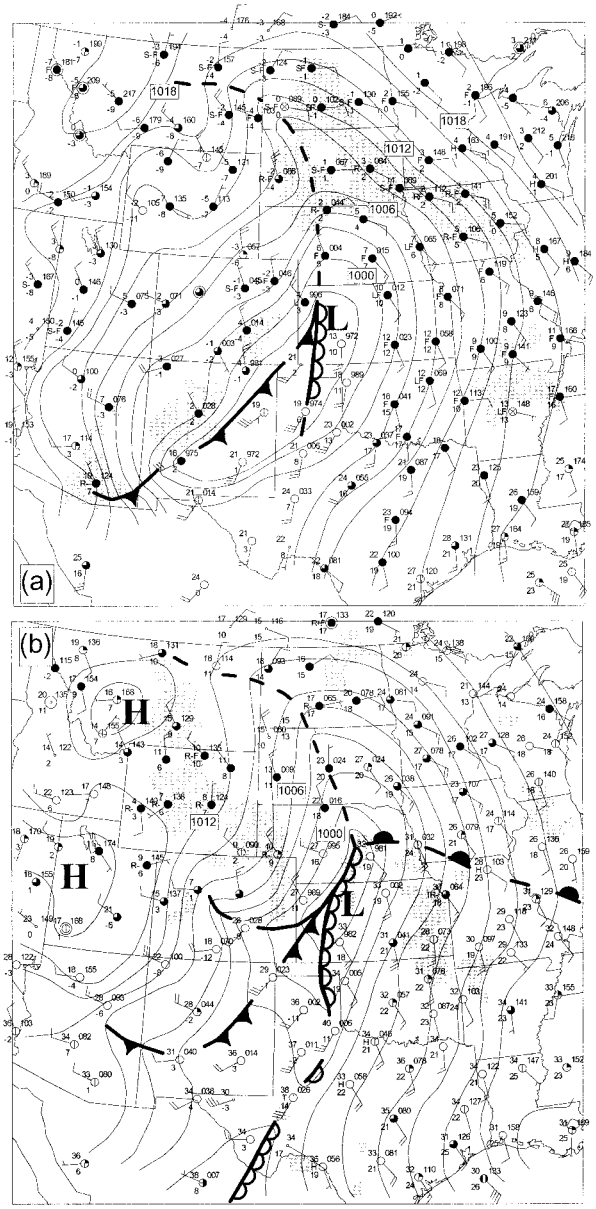

FIG. 1. Surface maps showing sea level pressures (solid lines labeled in hPa), surface features (conventional symbols), stations reports (conventional plotting), and regions of precipitation (shaded areas enclosing the lowest-level radar echo from the National Radar Summary) for (a) the Norwegian-type cyclone at 1800 UTC 9 Nov 1998, and (b) the CFA-type cyclone at 0000 UTC 18 Jun 1998. The solid line in (b) represents a secondary cold front.

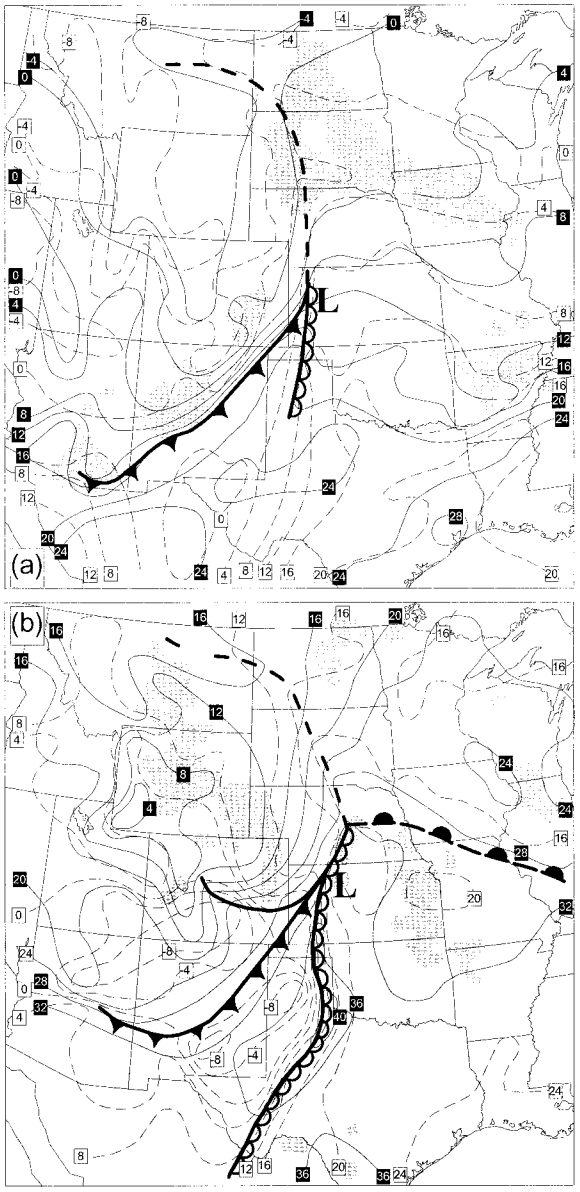

FIG. 2. As in Fig. 1 but showing surface temperatures (solid lines in °C) and dewpoint temperatures (dashed lines in °C).

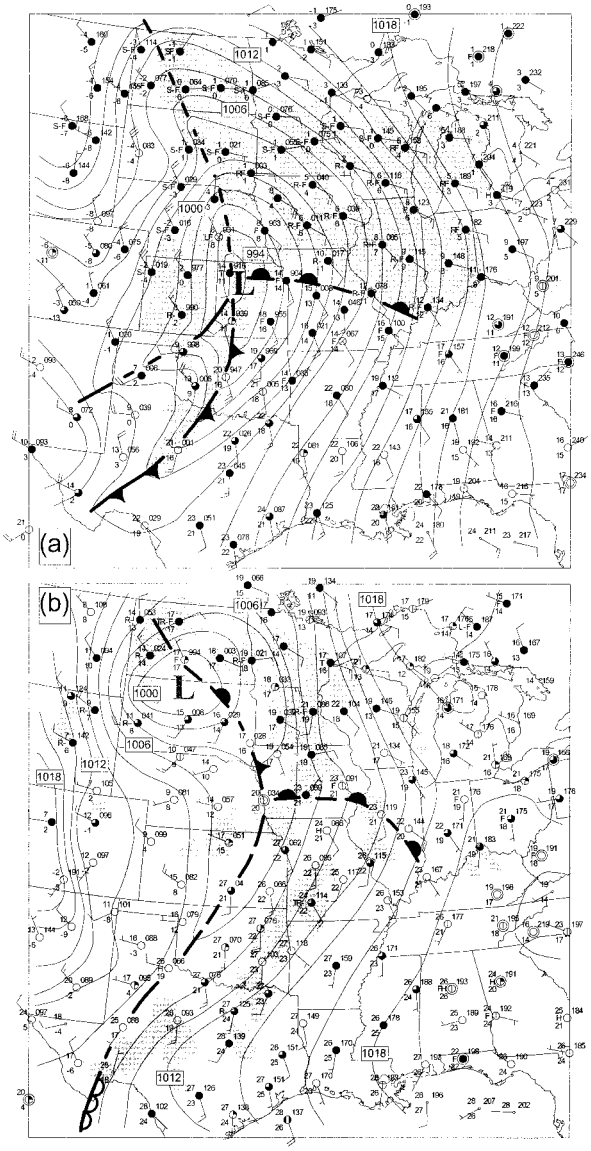

FIG. 3. As in Fig. 1 but for (a) The Norwegian-type cyclone at 0200 UTC 10 Nov 1998, and (b) the CFA-type cyclone at 1200 UTC 18 Jun 1998. The solid line in (a) represents a secondary cold front.

type cyclone had a secondary cold front confined to the east slopes of the Rockies and located west of the Pacific cold front, and a developing weak warm front east of the low pressure center.

Figure 2 shows the surface temperature and dewpoint analysis for both cyclones during their initial stages. The dryline is drawn in the middle of the dewpoint gradient, because we have found that in synoptic-scale analyses the pressure trough usually coincides most closely with the middle of the dewpoint gradient. Comparing Figs. 1 and 2 one can see that the lee trough/dryline had a stronger temperature, pressure, and moisture signature in the CFA-type cyclone than in the Norwegian-type cyclone. However, the Pacific cold front of the CFA-type cyclone had a weaker temperature gradient than the Norwegian type. Since the CFA-type cyclone occurred in June, and the Norwegian type in November, the average surface temperatures were much higher in the CFA-type cyclone. There is a hint of a rainband along the Pacific cold front in the Norwegian-type cyclone, but there is no precipitation associated with the Pacific cold front in the CFA-type cyclone.

b. Developing stage

Figures 3 and 4 show surface features for the Norwegian-type cyclone at 0200 UTC 10 November 1998, and for the CFA-type cyclone at 1200 UTC 18 June

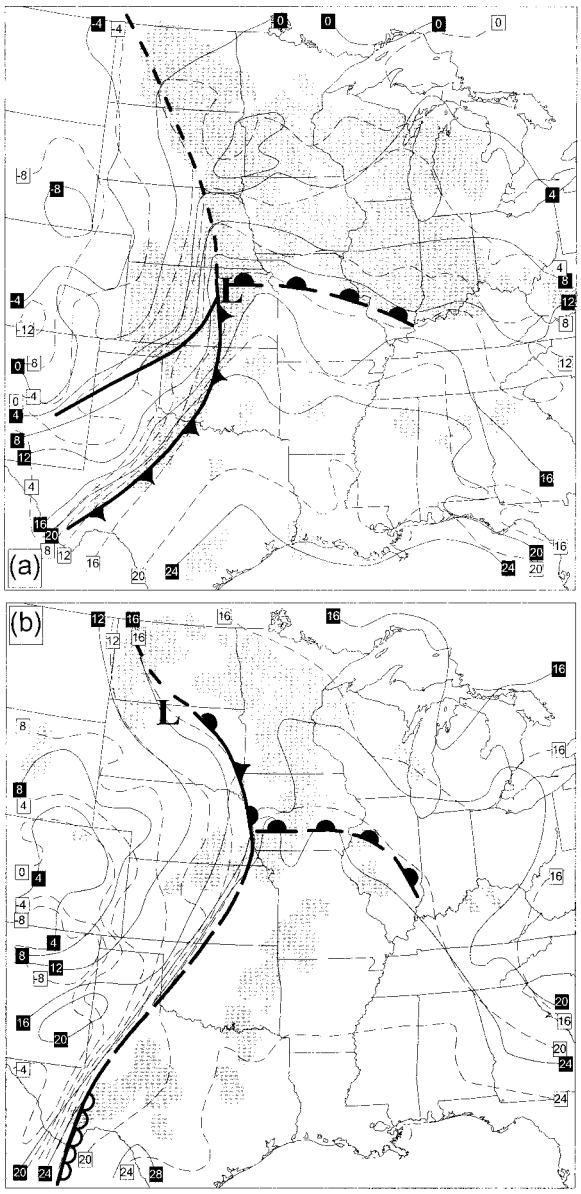

FIG. 4. As in Fig. 3 but showing surface temperatures (solid lines in °C) and dewpoint temperatures (dashed lines in °C).

1998. This is 8 h after the initial stage discussed above for the Norwegian-type cyclone, and 12 h after the initial stage of the CFA-type cyclone. Although the two cyclones looked very similar in their initial stages, in their developing stages they begin to show distinct differences. The low pressure center of the Norwegian-type cyclone moved from only western to eastern Kansas, and deepened by about 5 hPa. In contrast, the low pressure center of the CFA-type cyclone had moved from the Nebraska–Kansas border northward along the inverted trough to the border of North and South Dakota, and it did not deepen. By its developing stage, the Pacific cold front of the Norwegian-type cyclone had reached the surface position of the lee trough/dryline. Because the surface pressure trough from this time forward is a signature of the standard tipped-backward Pacific cold front (rather than the lee trough), we analyze the surface feature as a cold front at 0200 UTC (Fig. 3) and subsequent times, rather than as a trough. In the CFA-type cyclone, the Pacific cold front also reached the position of the lee trough/dryline at the time of its developing stage. However, because the surface pressure trough from this time forward is a signature of the remnant lee trough/dryline, we analyze the surface feature as a trough at 1200 UTC (Fig. 4) and subsequent times, rather than as a cold front.

The temperature and pressure gradients behind the Pacific cold front of the Norwegian-type cyclone are stronger than those behind the surface trough of the CFA-type cyclone. Also, the moisture gradient associated with the surface trough of the CFA-type cyclone is stronger than that associated with the Pacific cold front of the Norwegian-type cyclone. Of course, some of the pressure and temperature differences between the two storms are likely related to the different seasons during which the storms occurred (late spring/early summer for the CFA-type cyclone, and fall for the Norwegian-type cyclone). However, as will be shown, the basic structural difference between the two storms is not dependent on seasonal differences.

During their developing stages there are also important differences in the distribution of precipitation between the two cyclones. Note that the station reports do not always agree with the area of precipitation given by the radar coverage. This is not unusual since some radar echoes can be virga, the precipitation may be showery, and the National Radar Summary can overestimate coverage through smoothing of the radar echoes. The precipitation associated with the Norwegian-type cyclone coincides with surface frontal features, as expected from the Norwegian model. There is a rainband coincident with the surface cold front, and a wide swath of precipitation north of and parallel to the warm front (Fig. 4a). In contrast, the precipitation in the CFA-type cyclone is not (in any obvious way) associated with the location of the surface front; instead it is mostly ahead of the surface trough. There is precipitation located north of the surface warm front, but the precipitation swath is more likely associated with the surface trough because its orientation is more parallel to the surface trough.

Since both cyclones were in their developing stages close to the synoptic times of 0000 and 1200 UTC, we can use standard upper-level maps at 500, 700, and 850 hPa, produced by the National Centers for Environmental Prediction (NCEP), to aid understanding of the differences between the two cyclones. These maps are shown in Figs. 5, 6, and 7. We have left unchanged the NCEP geopotential height analysis, but have provided our own subjective temperature analysis. Figures 5a, 6a, and 7a are for the Norwegian-type cyclone at 0000 UTC 10 November 1998, and Figs. 5b, 6b, and 7b are for

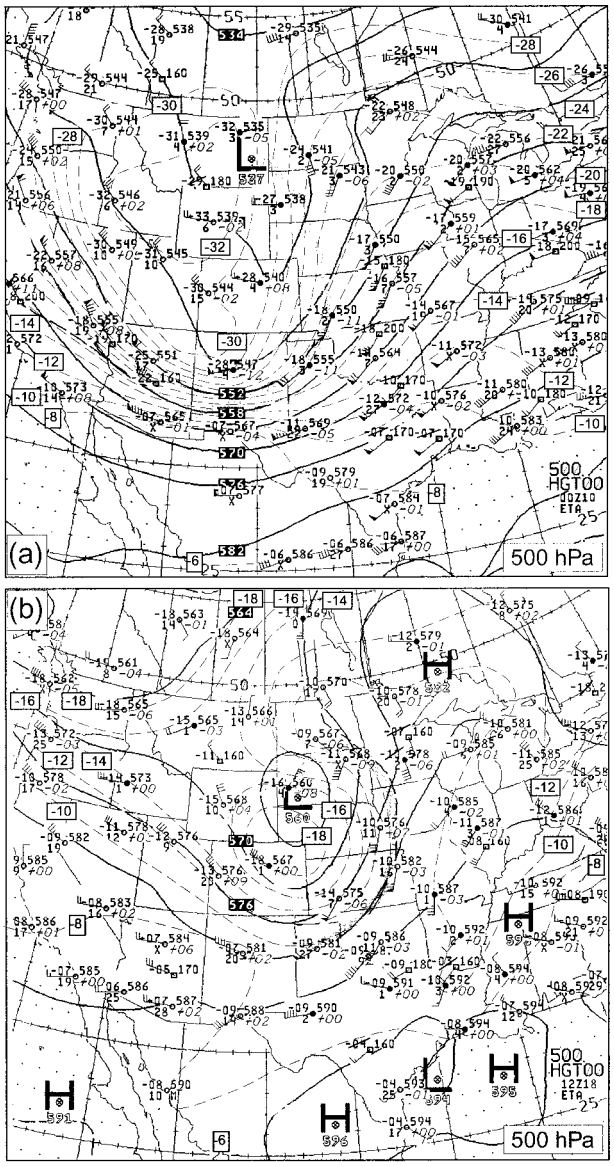

FIG. 5. 500-hPa geopotential heights (solid lines in dam), stations reports (conventional plotting), and temperatures (dashed lines in °C) for (a) the Norwegian-type cyclone at 0000 UTC 10 Nov 1998, and (b) the CFA-type cyclone at 1200 UTC 18 Jun 1998. The gray line marks the subjectively analyzed intersection of the Pacific cold-frontal surface with this pressure level.

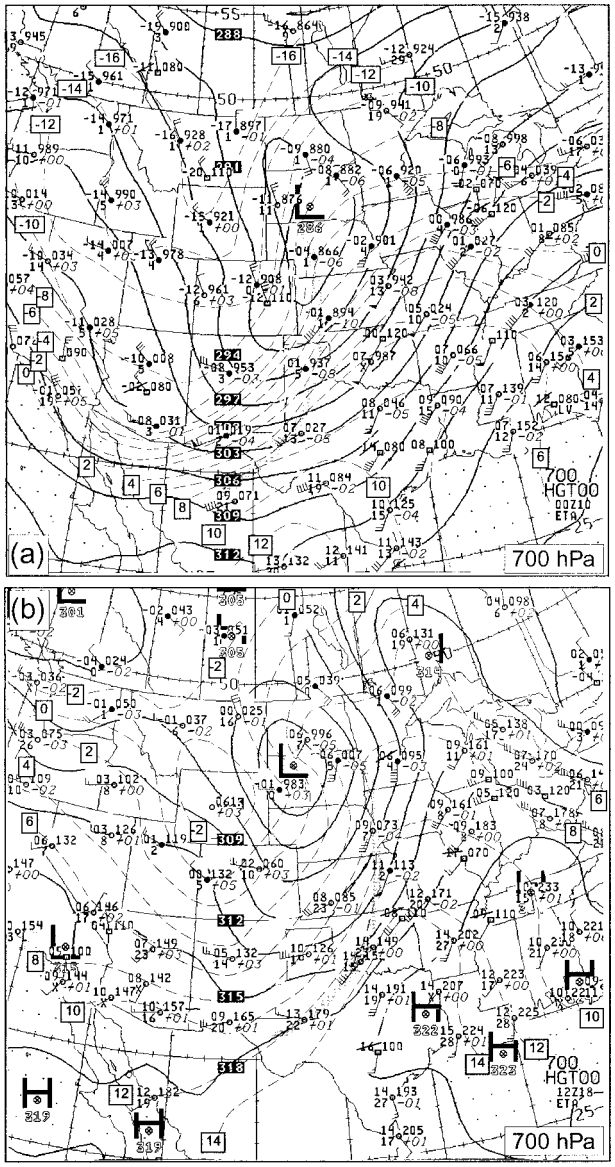

FIG. 6. As in Fig. 5 but for 700 hPa.

the CFA-type cyclone at 1200 UTC 18 June 1998. The subjectively-analyzed intersection of the Pacific cold frontal surface with each pressure level is shown by a shaded line.

There are considerable differences in the temperature and geopotential height fields at 500 hPa between the two cyclones in their developing stages. In the CFA-type cyclone the 500-hPa height minimum was over northwestern Nebraska, and the lowest temperatures at 500 hPa were south of this low pressure center over northeastern Colorado (Fig. 5). The Pacific cold front had swung around and away from the short-wavelength 500-hPa low center in an arc, with the strongest temperature gradients to the east of the 500-hPa low pressure center. In contrast, the height minimum at 500 hPa for the Norwegian-type cyclone was over eastern Montana, and the lowest temperatures at 500 hPa were centered to the southwest over northwestern Wyoming. A strong short wave moved through the long-wave trough at 500 hPa, where the largest pressure and temperature gradients were located. In summary, in the Norwegian-type cyclone the Pacific cold front at 500 hPa had not swung around the 500-hPa trough, but in the CFA-type cyclone it had. We should note, however, that, lacking a definitive mechanism for the formation of the CFA, it is not possible to ascertain whether these differences

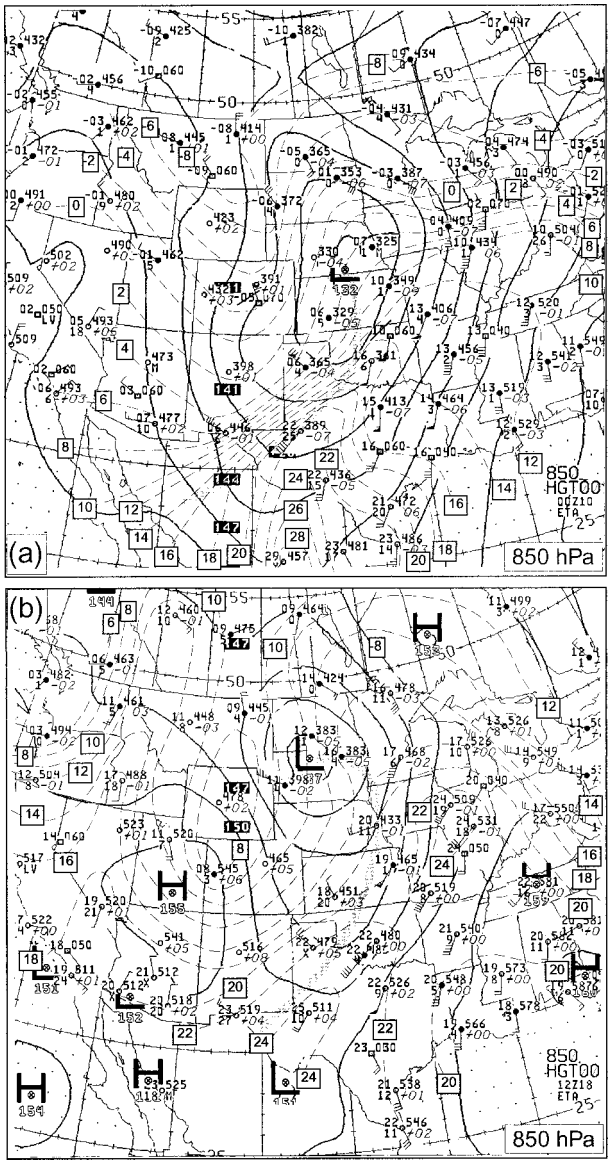

FIG. 7. As in Fig. 5 but for 850 hPa.

are directly relevant to whether or not a CFA formed in these two cases, or whether they reflect the natural variability of frontal structures and intensities of cyclones in this region.

At 700 hPa (Fig. 6) the low pressure centers and the centers of lowest temperatures for each of the two cyclones were at similar locations. However, the 700-hPa temperature gradient associated with the Pacific cold front of the Norwegian-type storm was about 2.7 K (100 km)$^{-1}$, while that associated with the Pacific cold front of the CFA-type cyclone was about 1.8 K (100 km)$^{-1}$. Also, an important difference can be seen in the locations of the Pacific cold front at 700 hPa relative to the 700-hPa low pressure centers (Fig. 6). As in the case for 500 hPa, the Pacific cold front at 700 hPa in the CFA-type cyclone had swung around the low pressure center in an arc to the east, but in the Norwegian-type cyclone the Pacific cold front at 700 hPa remained to the south of the low pressure center.

At 850 hPa the low pressure center of the Norwegian-type cyclone was located on the Kansas–Nebraska border, and the lowest temperatures were located northwest of the low center in northern Montana (Fig. 7). The 850-hPa center of the CFA-type cyclone was located farther northward on the North Dakota–South Dakota border, and the lowest temperatures at 850 hPa for the CFA-type cyclone were located to the southwest of its low pressure center. For the Norwegian-type storm the temperature gradient associated with the Pacific cold front at 850 hPa (Fig. 7) was much greater [5 K (100 km)$^{-1}$] than that of the CFA-type cyclone [1.8 K (100 km)$^{-1}$]. The Pacific cold front at 850 hPa advanced farther around the low pressure center for the CFA-type cyclone than for the Norwegian-type cyclone. The different positions of the Pacific cold fronts in relationship to the low pressure centers of the cyclones were associated with the different tilts of the upper-level troughs of the cyclones. The Norwegian-type cyclone was associated with a positively-tilted trough (a southwest–northeast tilt in the axis of the trough), while the CFA-type storm was associated with a negatively-tilted trough (a northwest–southeast tilt).

The locations of the low pressure centers and the Pacific cold fronts for the Norwegian-type cyclone and the CFA-type cyclone at the surface and at 850, 700, and 500 hPa are shown in Fig. 8. For the Norwegian-type cyclone (Fig. 8a), the most easterly position of the Pacific cold front was at the surface, and the front therefore tips westward (backward with height). For the CFA-type cyclone (Fig. 8b), the farthest eastward position of the Pacific cold front was in advance of the surface trough. The advancement of the cold front aloft ahead of the surface trough argues for showing the surface feature as a trough rather than as a cold front, although other possibilities for analyzing this nonclassical frontal structure are discussed in section 5 of this paper.

c. Mature stage

Surface features for the mature stage of the Norwegian-type cyclone at 1200 UTC 10 November 1998 are shown in Figs. 9a and 10a, and for the CFA-type cyclone at 0600 UTC 19 June 1998 in Figs. 9b and 10b. For the Norwegian-type cyclone the analyses of the developing stage and the mature stage are separated by 10 h, and for the CFA-type cyclone by 18 h.

By the mature stage, both cyclones had developed rainbands over 1800 km long and were producing severe weather over many states. However, the differences between the two cyclones are quite apparent. The Norwegian-type storm developed large pressure gradients around its low pressure center and a strong secondary trough in western Iowa, resulting in strong winds par-

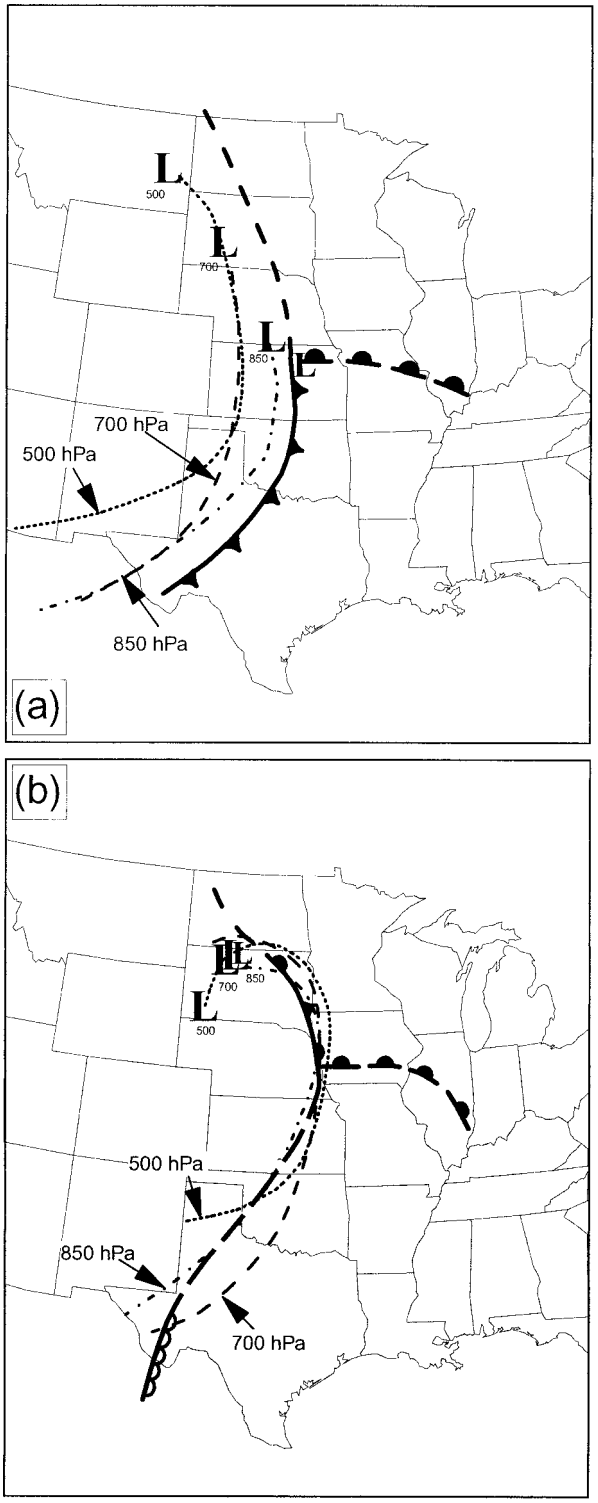

FIG. 8. Location of surface features and low pressure centers (conventional symbols), and the Pacific cold front and low pressure centers at 850 hPa (dash–dot line), 700 hPa (dashed line), and 500 hPa (dotted line) for (a) the Norwegian-type cyclone at 0000 UTC 10 Nov 1998 and (b) the CFA-type cyclone at 1200 UTC 18 Jun 1998.

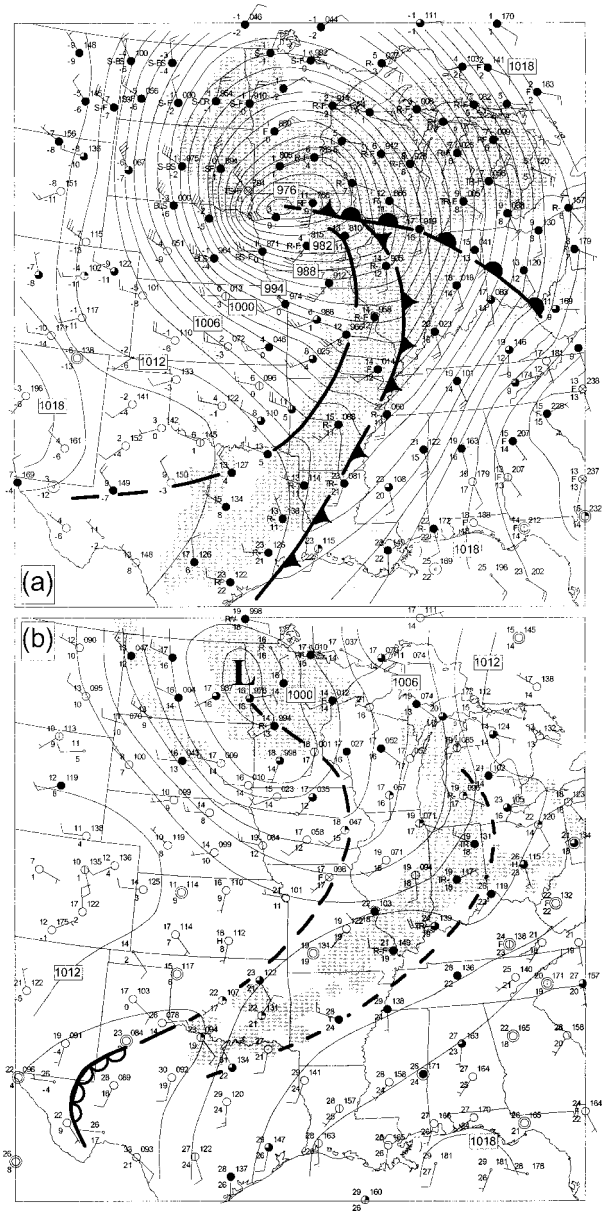

FIG. 9. As in Fig. 1 but for (a) the Norwegian-type cyclone at 1200 UTC 10 Nov 1998, and (b) the CFA-type cyclone at 0600 UTC 19 Jun 1998. The solid line in (a) represents a secondary cold front, and the leading dashed line in (b) represents a thunderstorm outflow boundary.

ticularly in the southwest quadrant of the low. A primary and a secondary surface cold front (solid heavy lines in Fig. 9a) are apparent in the pressure, wind, temperature, and dewpoint fields. The warm front is readily apparent in the wind (Fig. 9a), temperature, and dewpoint fields (Fig. 10a). In contrast, in the CFA-type cyclone, the surface warm front is no longer discernible in any of the fields. Also, the low pressure center of the CFA-type cyclone was not encircled by strong pressure gradients, and consequently, unlike the Norwegian-type cy-

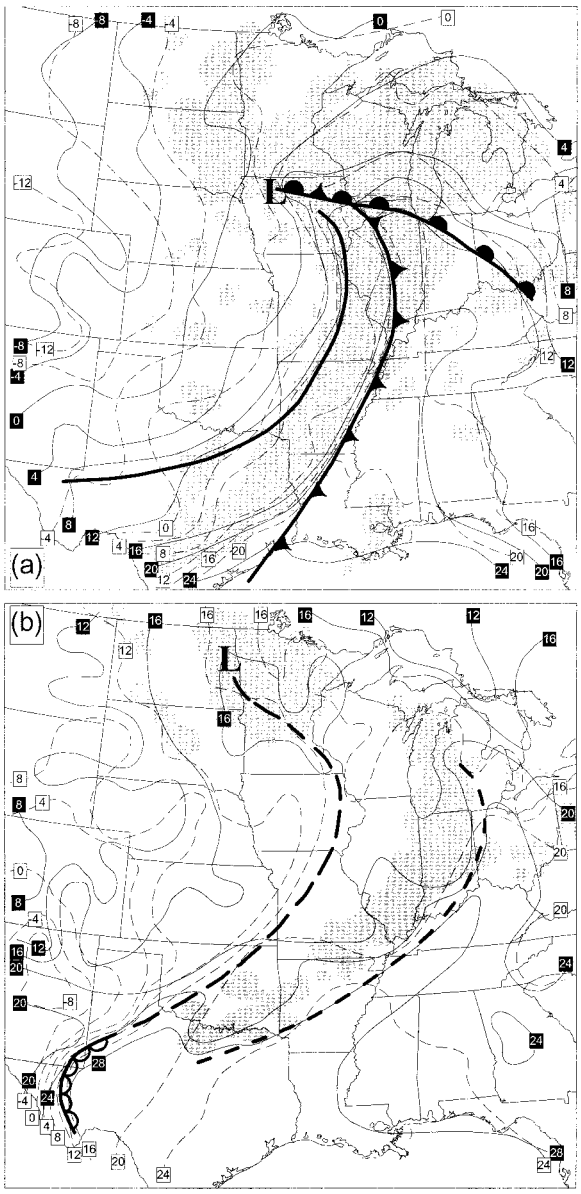

FIG. 10. As in Fig. 9 but showing surface temperatures (thin solid lines in °C) and dewpoint temperatures (thin dashed lines in °C).

clone, strong winds were not present. These differences are not necessarily related to the type of cyclone—the two cyclones are clearly of different intensity, which may or may not have a bearing on evolution of the Pacific cold front into a tipped-backward or tipped-forward orientation.

The most important and defining differences, seen in the surface analysis for the two cyclones, are in the nature of the surface trough/dryline and in the distribution of precipitation. In the developing stages of both cyclones (Figs. 3 and 4) their surface troughs, which extended south of the low centers into the southern Great Plains, displayed clear signatures in sea level pressure, surface temperature, and surface dewpoint. However, in the mature stage of the Norwegian-type cyclone, the surface cold front retained a clear signature in the surface fields, the corresponding surface trough in the CFA-type cyclone did not (Figs. 9 and 10). A surface trough is shown as a dashed line in Fig. 9b, with a short segment at its southern end drawn as a dryline. The location of this trough and dryline is consistent with where the National Weather Service (NWS) drew a surface cold front at this time. However, the only remaining significant signature of the once-robust lee trough and dryline is the dewpoint gradient collocated with the dashed line in Fig. 10b. The pressure trough is coincident with the dewpoint gradient north of Missouri, but it is poorly defined and lags behind the dewpoint gradient from Missouri southward—note that the minimum pressure in Kansas is probably not at the southeast corner of the state, but rather somewhere in the middle of the state. The discrepancy between the pressure and dewpoint signatures in the mature stage of the CFA-type cyclone is even more obvious in the model simulation (presented in the next section). In light of the evolution of the lee trough, the dashed line in Fig. 9 should be interpreted as a marker of the most clearly discernible remaining signature of the once-robust lee trough/dryline, namely, the dewpoint gradient.

Regarding the precipitation distribution, in the mature stage of the Norwegian-type cyclone the precipitation was aligned along the surface fronts (Fig. 9a), as it was in its developing stage (Fig. 3a). For example, in the Norwegian-type cyclone the long rainband associated with the surface cold front was parallel to and immediately behind the surface cold front. However, in the CFA-type cyclone only negligible precipitation was aligned along the surface trough. The significant precipitation in the CFA-type cyclone was aligned in an arc east of and 200–500 km ahead of the surface trough. Prior to the time of the analysis shown in Fig. 9b, convection was strong enough that the outflow from thunderstorms produced an extensive cold outflow boundary on the surface (heavy dashed line in Figs. 9b and 10b) at the leading edge of the arc of precipitation.

Diagnoses of the upper-level structure of the two cyclones at earlier times (Figs. 5–8) indicate that the differences in precipitation distribution are related to the differences in the upper-level structures of the cyclones. However, conventional upper-air analysis, which is confined to two daily observation times at the standard pressure levels of 850, 700, 500, 300, and 250 hPa, is insufficient to show details of the upper-level structure. Therefore, to better diagnose the differences in structure between the two cyclones and the striking difference in precipitation distribution, simulations from a mesoscale model were employed.

3. Mesoscale model simulations

The Pennsylvania State University–National Center for Atmospheric Research fifth-generation Mesoscale

Model (MM5; Dudhia 1993; Grell et al. 1994) was used to simulate both the Norwegian-type and the CFA-type cyclones described in section 2. The MM5 model is a nonhydrostatic, primitive equation model that uses the terrain-following sigma vertical coordinate, and a rectangular grid on a conformal map projection.

We ran the MM5 model simulation of the Norwegian-type cyclone after the occurrence of the cyclone. Specific physical parameterizations for this simulation include a high-resolution planetary boundary layer (PBL) scheme (Blackadar 1979), the Grell (1993) cumulus parameterization, and an explicit cloud microphysical scheme (including separate treatment of cloud water, rain, cloud ice, and snow) implemented by Reisner et al. (1993). The model grid for this simulation consisted of a 30-km grid resolution over a 2400 km × 3000 km domain. The simulation was initialized at 0000 UTC 10 November 1998, using NCEP gridded analyses as a first guess, enhanced with all available surface and upper-air data via a Cressman-type objective analysis scheme.

The MM5 model simulation of the CFA-type cyclone was run as a real-time forecast by the National Severe Storms Laboratory (NSSL). This simulation differed from that of the November case in that it used the Kain and Fritsch's (1990) cumulus parameterization, it was run on a 32-km grid, initialized at 0000 UTC 18 June 1998, and gridded data from NCEP's real-time Eta forecast model were used for initial and boundary conditions, instead of observationally-based gridded analyses.

a. MM5 model 1000–500-hPa thickness field

Previous studies (Hobbs et al. 1990) have shown that the 1000–500-hPa thickness field can indicate whether the leading edge of the tropospheric cold air mass is located behind or in advance of a surface front, and therefore can help in locating the leading edge of the Pacific cold front relative to surface fronts. Figure 11a shows MM5 model results of sea level pressure and 1000–500-hPa thickness for the Norwegian-type cyclone for model hour 12, valid at 1200 UTC 10 November 1998. The heavy dashed line shows the location in Fig. 11a of the surface Pacific cold front. Figure 11b shows the model results for sea level pressure and 1000–500-hPa thickness for the CFA-type cyclone for model hour 30, valid at 0600 UTC 19 June 1998. The position of the surface cold front in Fig. 11a is apparent from the strong surface trough in the pressure field. In the case of the CFA-type cyclone there is only a remnant of the original lee trough/dryline at this time in the model simulation, represented by the dashed line in the Fig. 11b. This is similar to the observations (Figs. 9b and 10b). This remnant is characterized much more by a moisture gradient (not shown) than by any clearly defined pressure trough. There is a weak surface pressure trough coincident with the dashed line from Missouri northward, but not south of Missouri where the pressure trough lags behind the moisture boundary even

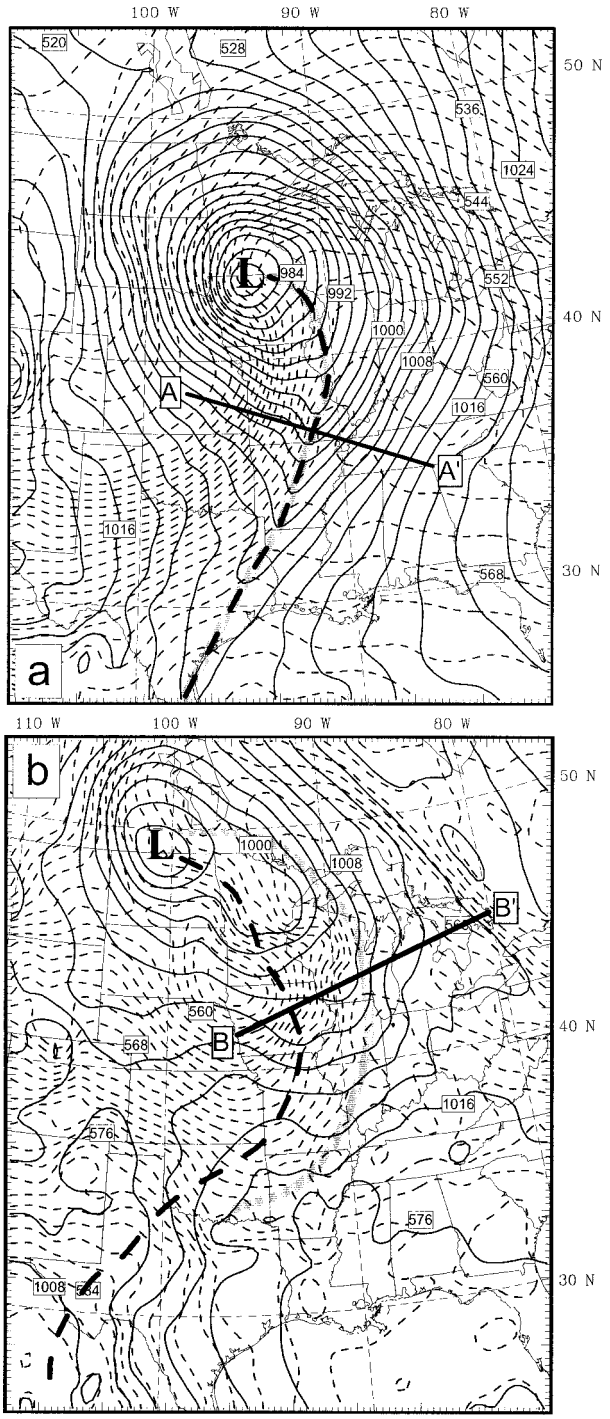

FIG. 11. Sea level pressures (solid line in hPa), 1000–500-hPa thicknesses (dashed lines in dam), and locations of the thickness front (gray line) from MM5 model simulations of (a) the Norwegian-type cyclone valid for 1200 UTC 10 Nov 1998, and (b) the CFA-type cyclone valid for 0600 UTC 18 Jun 1998. The lines AA′ and BB′ show the locations of the cross sections shown in Figs. 12a and 12b, respectively.

more than it did in the observations. Therefore, as in the observations (Figs. 9b and 10b), the dashed line in Fig. 11b should be taken as the location of the remnant of the lee trough/dryline, the signature of which is now much more apparent in dewpoint than in sea level pressure. Comparison of the actual sea level pressure field for the Norwegian-type cyclone (Fig. 9a) with the sea level pressure field from the model simulation (Fig. 11a) shows that the latter accurately captured the position of the surface cold front and the pressure field. Similarly, comparison of the actual sea level pressure field and the location of the surface moisture gradient for the CFA-type cyclone (Fig. 9b) with the sea level pressure field and location of the surface moisture gradient from the model simulation (Fig. 11b), shows that the model simulation also accurately captured these features.

The leading edge of the eastward-moving gradient in thickness, which marks the sudden decrease in the average temperature in the atmosphere, is marked in Figs. 11a and 11b by a heavy gray line. Hobbs et al. (1990) referred to such features as thickness fronts. In the Norwegian-type cyclone, the thickness front lies along the surface cold front, indicating that the surface cold front is the farthest forward extent of the cold air mass. However, in the CFA-type cyclone the thickness front is positioned in an arc (similar to the precipitation pattern in Fig. 9b) located ahead of the surface trough. This indicates that in the CFA-type cyclone the farthest forward extent of the cold air mass is in advance of the surface trough and in proximity to the precipitation arc. To ascertain more accurately the vertical structures of both cyclones, and to clarify the relationships of the positions of the Pacific cold fronts to the precipitation patterns, we will now examine vertical cross sections from the MM5 model simulations.

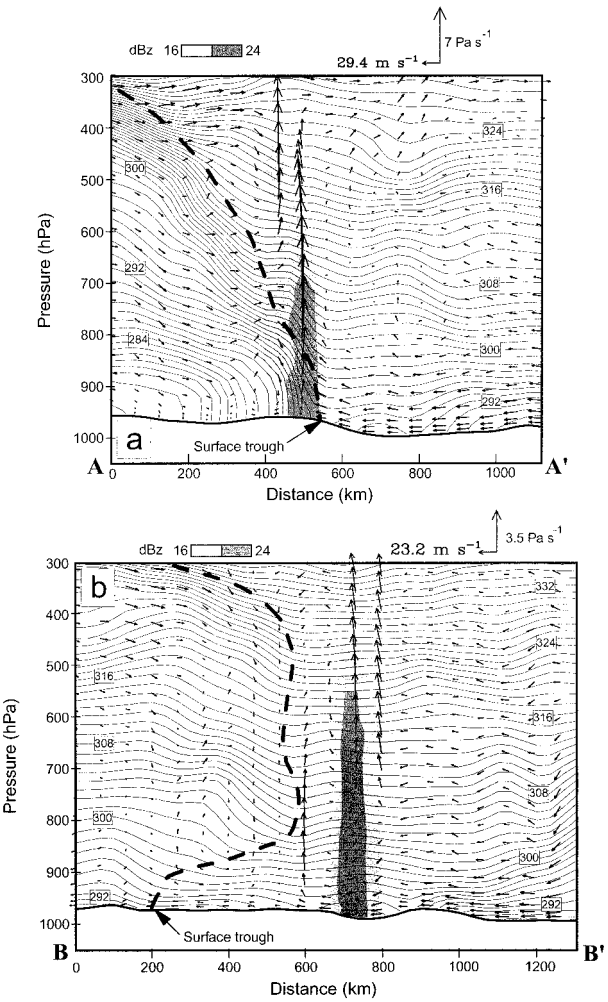

FIG. 12. Vertical cross sections from the MM5 model showing potential temperatures (solid lines in K), radar reflectivities (see figure legend), and winds in the cross section (see figure legend) relative to the speeds of the rainbands associated with the Pacific cold front along (a) the line AA′ in Fig. 11a, and (b) the line BB′ in Fig. 11b. The Pacific cold front is marked by the heavy dashed line. (a) The Norwegian-type cyclone is valid for 1200 UTC 10 Nov 1998. (b) The CFA-type cyclone is valid for 0600 UTC 18 Jun 1998.

b. MM5 model cross sections

The location of the MM5 model cross section through the Norwegian-type cyclone is shown by the line labeled AA′ in Fig. 11a, and for the CFA-type cyclone by the line labeled BB′ in Fig. 11b. The locations of the cross sections were chosen to be perpendicular to the Pacific cold front, and in the case of the CFA-type cyclone in a manner that maximized the distance between the surface trough and the CFA. The corresponding cross sections are shown in Fig. 12a for the Norwegian-type cyclone and in Fig. 12b for the CFA-type cyclone. In both cross sections the 2D circulation vectors normal to the cross section are shown relative to the motion of the rainband associated with the corresponding Pacific cold front. Contours of potential temperature are also shown. In both cross sections the leading edge of the forward-moving baroclinic zone is marked by a heavy dashed line, which is the location of the Pacific cold front.

The vertical profile of the Pacific cold front is quite different for the two cyclones. Whereas the front slopes westward (backward) throughout the troposphere in the Norwegian-type cyclone, it slopes eastward (forward) in the lower troposphere in the CFA-type cyclone. The strongest concentrated vertical velocity (and associated rainband) is along the surface cold front in the Norwegian-type cyclone. In the CFA-type cyclone, however, these features are located ~500 km ahead of the surface trough, at or ahead of the leading edge of the Pacific cold front aloft. The relative winds in each cross section show that in both types of cyclones the Pacific cold front marks the border between cold air that is generally advancing and sinking, and the warm air that is generally rising ahead of the Pacific cold front. In both cyclones, the strongest vertical velocities are con-

TABLE 1. Results of 1-yr study of cyclones (15 Sep 1994–15 Sep 1995) that maintained closed surface lower pressure centers for at least 24 h and produced precipitation in the United States east of the Rocky Mountains. Percent values refer to the fraction of total storms for that season.

Season	Total no. of cyclones	CFA-type cyclones	Norwegian-type cyclones	Indeterminate-type cyclones	No. of cyclones with lee troughs
Fall (Sep–Nov)	11	4 (36%)	3 (27%)	4 (36%)	11 (100%)
Winter (Dec–Feb)	19	8 (42%)	4 (21%)	7 (37%)	15 (79%)
Spring (Mar–May)	27	17 (63%)	4 (15%)	6 (22%)	24 (89%)
Summer (Jun–Aug)	13	3 (23%)	5 (38%)	5 (38%)	12 (92%)
Full year total	70	32 (46%)	16 (23%)	22 (31%)	62 (89%)

centrated at or just in advance of the most-forward position of the Pacific cold front.

In the CFA-type cyclone the arc-shaped rainband began when the Pacific cold front reached the position of the lee trough/dryline and moved aloft in advance of the surface trough. The arc-shaped rainband then continued to move eastward, as much as 500 km ahead of the surface trough but approximately at the leading edge of the Pacific cold front aloft. We use the qualifier ''approximately'' because the arc-shaped rainband had actually moved ~150 km ahead of the CFA at the time of the cross section shown in Fig. 12b. This somewhat loose connection between the CFA and the rainband is due to the influence in the model of the precipitation-induced cold pool, which moves at a speed that is not necessarily the same as that of the CFA. Over time, the band may move ahead of the CFA, but then usually either slows down or weakens and reforms at the CFA, maintaining a mean position that is close to that of the CFA because that is where the externally applied lifting creates a favored location for convective maintenance (Stoelinga et al. 2000). Note that although the band is somewhat ahead of the CFA, a column of enhanced lifting remains locked to the CFA.

4. Frequency of occurrence of the two cyclone types

We have described two types of cyclones that can develop east of the Rocky Mountains when a Pacific cold front moves over the Rockies and intersects a lee trough/dryline. The Pacific cold front can stay on the surface (a Norwegian-type cyclone) or it can move aloft over the stable layer east of the lee trough/dryline (a CFA-type cyclone). In this section we provide information on the frequencies of occurrence with which each of these two types of cyclone occurred in a 1-yr period. This information was obtained by studying 70 cyclones that occurred in the United States east of the Rockies from 15 September 1994 through 15 September 1995, and using data that is routinely available to forecasters.

a. Criteria for classification of the two cyclone types

Subjective analyses of temperature, dewpoint, and pressure were performed on surface and upper-level charts provided by NCEP. For each cyclone the positions of the fronts at the surface, 700 hPa, and 500 hPa were compared with the positions of rainbands as they appeared on the NWS radar composites. A front located above the surface was classified as a CFA if it had a temperature gradient of at least 1 K (100 km)$^{-1}$, and if it marked the leading edge of an advancing zone of cold advection aloft located ahead of the surface trough. For those cases in which frontal features (especially the CFA) could not be analyzed definitively from horizontal maps, soundings were used to construct vertical cross sections of temperature and/or equivalent potential temperature. For those cases in which fronts were readily identified from upper-level charts, the position of the front at 500 or 700 hPa served as a proxy for the leading edge of the CFA; cross sections of the vertical structures showed this to be a reasonable approximation.

If a rainband was coincident with a surface cold front, and the cold front at 700 or 500 hPa remained behind the surface front, the cyclone was classified as Norwegian type. If at some stage in the development of the cyclone a rainband was coincident with a CFA at 500 or 700 hPa, it was classified as CFA type. If neither of these two sets of conditions were met, the cyclone was classified as indeterminate. Since we classified a cyclone as CFA type only if there was a clear indication of an advancing zone of cold advection aloft ahead of the surface trough, it is likely that the percentage of CFA-type cyclones derived by this method is, if anything, an underestimate.

b. Results and interpretations

The results of this study are shown in Table 1. Overall, 32 (or ~46%) out of the 70 cyclones were classified as CFA type and 16 (or ~23%) as Norwegian type. Thus, for those cyclones that could be classified in this way, there were twice as many CFA-type cyclones as there were Norwegian type.

Several factors account for the significant number (22 out of 70, or 31%) of the cyclones that were classified as indeterminate. In some cases, the Pacific cold front remained approximately vertically stacked over the surface trough, and a rainband was coincident with both. Since, in these cases, the error due to station spacing made it impossible to classify the frontal surface as tilted slightly forward or backward, the cyclones were clas-

sified as indeterminate. Some storms were extremely weak and produced either little precipitation or disorganized rainbands, despite maintaining a closed low pressure center at the surface for 24 h or more. Also, the precipitation associated with some of the summer cyclones was widespread and disorganized, rather than banded. Since the classification of cyclones in this study depended upon the association of readily-identifiable rainbands with well-defined fronts, these last two types of cyclones were also placed in the indeterminate category.

For classification by season we use the climatological definitions of the season, namely, winter (Dec–Feb), spring (Mar–May), summer (Jun–Aug), and autumn (Sep–Nov). Table 1 shows that for the year studied, CFA-type cyclones were more common than Norwegian type in all seasons except summer. The results also indicate that cyclones were most likely to be CFA type during spring, at least for the 1 yr studied. This could be because spring is the peak season for cyclogenesis over the southern Rockies (Reitan 1974), and in this season a statically stable (but potentially unstable) atmosphere is common east of the lee trough due to the inflow of moist low-level air from the Gulf of Mexico underneath a southwesterly flow of very warm, dry air originating over the high terrain to the west.

Table 1 shows that lee troughs occurred in 62 out of the 70 or 89% of the storms studied. Thus, lee troughs should be an important component of any conceptual model of cyclone structures in the central United States.

5. Discussion

a. 1-yr climatology

The climatology presented in the previous section demonstrates that, for at least 1 yr, CFA-type cyclones were more common in the central United States than Norwegian-type cyclones. However, considering the subjective nature of the study, the overabundance of CFA-type cyclones (relative to Norwegian type) could fall within the error bars associated with subjectivity. Furthermore, the limited time period of the study and the potential for large year-to-year variability precludes any extension of that conclusion to central United States cyclones in general. It is not the goal of this study to show, or even suggest, that CFA-type cyclones are the more common type of cyclone in the central United States. What this study is intended to show is strong evidence that CFA-type cyclones are common enough in this region to warrant consideration by forecasters on a daily basis.

It should be noted that although the 1-yr study indicated a minimum of CFA-type cyclones in summer, the CFA-type cyclone described in sections 2 and 3 of this paper occurred in the early part of the climatologically-defined summer period (Jun–Aug). Strong Pacific cold fronts traversing the central and southern Rockies become less common in summer, but when they do occur they often meet an air mass with high convective available potential energy (CAPE) east of the lee trough/dryline. If a CFA develops with such storms, the potential for severe weather along the CFA is significant.

b. Temperature gradients associated with a CFA

Bluestein (1993) suggested that the minimum gradient for a front should be ''an order of magnitude or more greater than the typical synoptic-scale strength of 10 K per 1000 km.'' If this requirement was applied to the typical temperature gradients associated with a CFA, then they would not qualify as fronts. However, this criterion is relevant only to surface fronts, where friction and the constraint on vertical velocity allow for stronger temperature gradients than are observed aloft. Cold fronts aloft, with gradients of only 1–2 K $(100\ \text{km})^{-1}$, can produce significant rainbands. For example, Locatelli et al. (1989) discuss a case with a weak baroclinic zone at 700 hPa [1.3 K $(100\ \text{km})^{-1}$] whose leading edge was collocated with a rainband. Hobbs et al. (1990) describe an intense CFA rainband on 13 March 1986 that was associated with a temperature gradient of 1.5 K $(100\ \text{km})^{-1}$ at 700 hPa. NCEP's Nested Grid Model (NGM) 12-h forecast for this case showed an extensive region of upward motion with a magnitude >6 cm s^{-1} at 700 hPa along the CFA. Two other cases described by Hobbs et al. (1990) from the same study show similar patterns: a temperature gradient on the order of 1 K $(100\ \text{km})^{-1}$, a rainband aligned along the leading edge of the cold advection, and model-predicted upward motion at 700 hPa along the CFA. Locatelli and Hobbs (1995) suggested that the world-record rainfall rate produced by the Holt, Missouri, storm of 22 June 1947 was associated with a CFA with a temperature gradient of 1.2 K $(100\ \text{km})^{-1}$. As such, the features referred to in this and other papers as CFAs should be classified as cold fronts.

c. Surface analysis of CFA-type cyclones

As the Pacific cold front moves aloft and eastward in a CFA-type cyclone, the surface trough continues to move eastward but trails behind the CFA. For the CFA-type cyclone described in section 2 of this paper, the surface trough had a discernible temperature and dewpoint gradient associated with it in the hours immediately after the Pacific cold front overtook the lee trough (Fig. 4b). As the CFA-type cyclone approached the mature stage in its development (Fig. 10b), the pressure and temperature signature of the surface trough diminished, but the moisture structure did not. Other CFA-type cyclones have been described that have surface troughs with similar attributes (Hobbs et al. 1990; Businger et al. 1991). In other cases, there can be a temperature maximum and strong pressure signal along the trailing trough in a CFA-type cyclone (Hobbs et al.

1990; Sienkiewicz et al. 1989; Locatelli et al. 1989, 1995, 1998; Martin et al. 1990; Castle et al. 1996; Stoelinga et al. 2000). Further complicating the structure of the trailing trough are secondary cold fronts and arctic fronts that can move from the north and west into the northern portion of the trailing trough producing a cold-frontal signature in temperature along the trough.

The increasing recognition of the CFA-type cyclone as a common feature in the central United States carries with it the need for a meaningful and consistent way to analyze surface weather maps in situations where CFA-type cyclones are present, so that forecasters, as well as nonexpert users of weather maps, can anticipate the potential for organized significant weather ahead of the surface trough. The two key issues are

- Should CFAs be shown on surface weather maps?
- Should the trailing surface trough in CFA-type cyclones be shown on surface weather maps?

We address these questions below by discussing several possibilities in terms of their advantages and disadvantages. The final choice should remain in the hands of operational weather analysts and the forecasting community.

The approach taken by the authors for surface analysis of the CFA-type cyclone in the present paper was a conservative one: we chose not to mark the CFA, and to mark the trailing surface trough with the standard trough (dashed line) symbol. However, we acknowledge that this approach does not fully satisfy what we believe is a need for surface weather maps to bring more immediate attention to the fact that a CFA is present in CFA-type cyclones, with the various attendant implications for significant weather.

With regard to the first question above, CFAs were once analyzed on surface weather charts with a standard symbol consisting of a line with spaced open triangles. This practice was discontinued around 1950, after which the CFA symbol was rarely (if ever) seen on surface weather charts, either in operational or research settings. However, Hobbs et al. (1990) presented several cases of CFA-type cyclones in which they indicated the presence of a CFA with the traditional symbol on the surface weather map. Since then, other researchers have returned to the practice of analyzing CFAs on surface weather maps (e.g., Neiman et al. 1998). The advantage of marking CFAs on surface maps is that it immediately draws attention to the significant weather that is likely to be expected at that location, rather than at the surface trough. However, there are practical limitations to locating CFAs in an operational setting, particularly on surface weather maps prepared in between the standard upper-air times (0000 and 1200 UTC). A wide variety of information (discussed in more detail in the next subsection), including surface data, mesoscale model output, radar summaries, etc., must be integrated to identify the 3D structure of the Pacific cold front and determine if a CFA is present.

With regard to the second question, NCEP has dealt with the trailing surface trough in CFA-type cyclones in a number of different ways in their operational surface analyses. Prior to the arrival of the Pacific cold front, the lee trough is typically analyzed as a trough (dashed line) and/or a dryline (line with adjacent open scallops), depending on the moisture characteristics. However, in CFA-type cyclones, after the Pacific cold front overtakes the lee trough, different analysis approaches have been used operationally. The trough or dryline is often converted into a surface cold-frontal symbol, as was done in the NCEP surface analysis for the CFA-type cyclone of 18–19 June 1998 described in this paper. The trailing surface trough is also sometimes left unchanged as a trough or dryline. On rare occasions it is drawn as an occluded front.

In research studies, the most common symbology used for the trailing surface trough in storms that were recognized as CFA-type cyclones is to retain the trough symbol (dashed line) after the Pacific cold front overtakes the lee trough and its leading edge moves aloft (e.g., Hobbs et al. 1990; Neiman et al. 1998; Stoelinga et al. 2000; and the present paper). In the series of papers based on the University of Washington's studies of storms that occurred during the 1992 Storm-scale Operational and Research Meteorology-Fronts Experiment Systems Test (STORM-FEST) project (Martin et al. 1995; Wang et al. 1995; Locatelli et al. 1995; Castle et al. 1996; Locatelli et al. 1998), the lee trough/dryline was termed a ''drytrough'' and it was indicated on surface weather maps by a line with spaced open scallops both prior to and after it was overtaken by the Pacific cold front.

The advantages and drawbacks of each of the possible symbols for marking the trailing surface trough (cold front, trough, dryline, occluded front, or drytrough) on operational surface weather maps are discussed below.

1) COLD FRONTAL SYMBOL

Forward-tilted cold fronts have been observed in a variety of meteorological contexts (Hardy et al. 1973; Steenburgh and Mass 1994; Schultz and Steenburgh 1999), of which the CFA in the central United States is one type. They are dynamically plausible as long as the front is more aptly described as a first-order discontinuity in temperature rather than a zero-order discontinuity. Therefore, it is not unreasonable to analyze the trailing surface trough in a CFA-type cyclone as a surface cold front, even though it does not mark the surface position of a standard tipped-backward cold-frontal surface. However, because the Norwegian model for fronts and cyclones is so firmly implanted in the minds of many meteorologists, any feature marked on a map as a surface cold front naturally leads one to look for significant weather along that boundary, rather than ahead of it. Of course, this drawback would be mitigated if the CFA itself were also shown on surface weather

maps. The drawback could be mitigated more subtly by adding a category for a forward-tipped cold front to the frontal numbering system used at operational centers like NCEP.

2) TROUGH SYMBOL

The trough symbol is also a reasonable choice to mark the trailing surface trough of a CFA-type cyclone. Use of this symbol, more so than with the surface cold frontal symbol, is consistent with the typical history of the trailing surface trough as being directly connected to the original Rocky Mountain lee trough. The trailing trough often more closely retains the thermal and dewpoint features of the original lee trough than of the Pacific cold front. The only problem with this symbol is that, like the cold frontal symbol, it does not draw attention to the possibility that a CFA may be present that could produce significant weather ahead of the surface trough. Again, this drawback could be mitigated by marking the CFA on surface weather maps.

3) DRYLINE SYMBOL

If the original surface trough is coincident with a zone of moisture gradient strong enough to be characterized as a dryline, then it would be as reasonable to retain the dryline symbol after it is overtaken by the Pacific cold front as it would be to retain the trough symbol if it were originally marked as a trough. Once the moisture gradient is weakened to the point where a dryline symbol is no longer warranted, it can be changed to a trough symbol.

4) OCCLUDED FRONTAL SYMBOL

The greatest advantage of using the occluded frontal symbol for the trailing surface trough in a CFA-type cyclone is that it immediately implies that two boundaries have met (the Pacific cold front and lee trough/dryline) and that the Pacific cold front may have advanced aloft ahead of the occluded front; this would draw attention to the possibility of significant weather ahead of the trailing surface trough. Use of the occluded front is not ideal since an occluded front is traditionally thought to arise from the overtaking of a warm front by a cold front. A lee trough/dryline may have the characteristics of a weak warm front prior to its interaction with a Pacific cold front (Martin et al. 1995; Stoelinga et al. 2000), but this is not always the case (Neiman and Wakimoto 1999). Strictly speaking, the overtaking of a lee trough/dryline by a Pacific cold front, in which the Pacific cold front moves aloft over the stable air east of the lee trough/dryline as a CFA, is not a classical occlusion. However, the process is analogous to the formation of a warm occlusion, in that a cold front overtakes a stable layer east of the lee trough/dryline (akin to a warm front) and moves aloft over that stable layer, leaving a trough on the surface that has thermal characteristics similar to an occluded front (typically a thermal maximum).

5) DRYTROUGH SYMBOL

The term drytrough was introduced by Martin et al. (1995) to draw attention to the fact that, on the synoptic scale, lee troughs and drylines are often coincident because the wind field associated with a lee trough helps set up the strong moisture gradient associated with a dryline. The drytrough symbol (a line with spaced open scallops) was introduced as a way to recognize this fact on a surface weather map. In that sense, the drytrough symbol was essentially suggested as a replacement for the standard dashed line used to indicate a lee trough in the lee of the Rocky Mountains. Therefore, the considerations in using the drytrough symbol for the trailing surface trough in a CFA-type cyclone are essentially the same as for using the standard lee trough symbol, with following additional considerations. First, there is the technical issue that a line with spaced open scallops has been reserved by the National Weather Service to represent a warm front aloft, presumably within a cold-type occlusion, although such a feature is never drawn on operational weather maps. Second, use of the drytrough term or symbol in place of the lee trough/dryline has not been generally adopted by the operational or research community to date, probably reflecting a general resistance to new frontal symbols or terminology. Therefore, the most acceptable choice for analyzing the trailing surface trough in a CFA-type cyclone would probably involve one of the three symbols suggested above (cold front, trough, or occluded front), which are already routinely used in various situations on surface weather maps.

d. Forecasting considerations

The standard approach to severe weather forecasting is to examine the three key ingredients that are necessary for deep moist convection—namely, instability, moisture, and a lifting mechanism—and a fourth ingredient, vertical wind shear, which influences the type of convection (Doswell 1987). The point of this paper is not to suggest a change to this basic approach. Rather, it is to call attention to a nonclassical frontal structure that may provide a lifting mechanism in addition to those normally considered.

To determine the location of the potential source of lifting associated with the Pacific cold front, the forecaster should track the true leading edge of the front as it moves over the Rocky Mountains and out over the Great Plains by examining its structure at multiple pressure levels and in vertical cross sections. This approach is illustrated by the two examples of cyclones described in sections 2 and 3 of this paper, where we showed that the severe weather was situated along the leading edge

of the Pacific cold front. In the case of the Norwegian-type cyclone, the leading edge of the Pacific cold front remained on the surface, but for the CFA-type cyclone the leading edge of the Pacific cold front was aloft in advance of the surface trough. In both cases, the Pacific cold front was the locus of severe weather.

Tracking the leading edge of the Pacific cold front after it has moved above the surface can be difficult, since upper-air analysis is available only every 12 h. Although the CFA may not produce a thermodynamic signature on the surface, it can produce a weak pressure and wind shift at the surface (Locatelli et al. 1997; Neiman et al. 1998; Neiman and Wakimoto 1999). Schultz and Doswell (2000) used filtered pressure analysis and pressure checks from surface stations to track the movements of surface troughs associated with upper-level mobile disturbances. Perhaps this method could be used to track the movement of the leading edge of the Pacific cold front.

Another way to track and predict the location of the leading edge of the Pacific cold front is to use mesoscale model forecasts. The full 3D model output, vertical cross sections cutting roughly perpendicular to the lee trough and Pacific cold front, as well as horizontal maps of temperature, temperature gradient, and temperature advection at several pressure levels in the lower troposphere, can be used to pinpoint the 3D structure of the Pacific cold front, and to help determine if the front is tipped backward or forward. As a simpler alternative, Hobbs et al. (1990) suggested using the location of the thickness front as an indicator of the position of the leading edge of the Pacific cold front in a CFA-type cyclone. As shown in sections 2 and 3 of this paper, the leading edge of the Pacific cold front is often apparent in the model-simulated thickness fields for both the Norwegian type and the CFA-type cyclones (Fig. 11), and its position relative to the surface trough can be identified. Ultimately the use of models for forecasting features related to CFA-type storms is subject to the same timing and intensity errors that are inherent in any model forecast. However, when the forecast model produces a CFA, the model precipitation fields tend to be more reliable in forecasting convection associated with the CFA than in forecasting other convective situations that are organized on smaller scales. This is because the models generally perform well at capturing synoptic-scale features. Therefore, if a CFA-type cyclone is recognizable in a model forecast, and the model also shows an extensive band of precipitation ahead of the surface trough, the development of extensive, squall-line-type severe weather is likely to occur along a CFA provided other environmental conditions conducive to severe weather are in place.

Quasigeostrophic (QG) diagnostics, as embodied in jet-streak dynamics, Q-vector diagnosis, or the ''omega equation,'' are often cited in forecast discussions or convective outlooks. While we have stated above that CFAs are a synoptic-scale feature, large-scale (e.g., QG) diagnostic methods are by no means the most useful tool for identifying CFAs. The reason for this is that while a CFA is synoptic scale in length, and it is generated by synoptic-scale deformation patterns, it is mesoscale in the cross-front direction. Stoelinga et al. (2000) concluded that for CFAs, the relevant scale on which key dynamical processes occur (in terms of generating vertical velocity) is best described as ''frontal scale,'' which is smaller than the scale at which QG theory is valid. Locatelli et al. (2002) found this to be true in another case study, and improvements gained by using the more accurate semigeostrophic diagnosis (in the context of the Sawyer–Eliassen equation) were offset by a lack of two-dimensionality of the CFA and its environment. Rather than relying on these balance-based diagnostic techniques to pinpoint the lifting associated with a CFA, we recommend that attention be directed at locating the CFA, and in considering the CFA as a potential trigger for severe weather.

6. Conclusions

In this paper we have arrived at the following principal conclusions:

- Two different types of cyclones can form when a Pacific cold front overtakes a lee trough/dryline east of the Rocky Mountains: the Norwegian-type cyclone and the CFA-type cyclone.
- The Norwegian-type cyclone is characterized by a Pacific cold front, the leading edge of which is on the surface south of the classical triple point.
- The CFA-type cyclone is characterized by a Pacific cold front, the leading edge of which is aloft and ahead of the surface trough (we refer to this as the cold front aloft or CFA).
- In both Norwegian type and CFA-type cyclones the locus of lifting and precipitation associated with the Pacific cold front is at the farthest forward extent of the frontal surface, regardless of whether that occurs at the surface or aloft.
- For the period 15 September 1994–15 September 1995, 46% of the 70 cyclones that occurred in the United Stated east of the Rockies were CFA-type cyclones, and 23% were Norwegian-type cyclones. The other 31% could not be clearly classified.
- Lee troughs were present in 89% of the cyclones that occurred in the 15 September 1994–15 September 1995 period.
- The 500–1000-hPa thickness field can be useful in locating the leading edge of the Pacific cold front, and in determining whether a cyclone is a Norwegian type or CFA-type cyclone.
- We recommend the adoption of a consistent and meaningful system for depicting on surface maps the frontal features (primarily the CFA and the trailing surface trough) associated with CFA-type cyclones in the central United States.

Acknowledgments. We thank Michael J. Brown for his help in map analysis. We also thank David Stensrud at NSSL for providing output from NSSL's real-time MM5 forecast system. This research was supported by Grant ATM-9106235 from the Mesoscale Dynamic Meteorology Program, Atmospheric Research Division, National Science Foundation. The National Center for Atmospheric Research, which is supported by the National Science Foundation, provided computing resources.

REFERENCES

Bjerknes, J., and H. Solberg, 1922: Life cycle of cyclones and the polar front theory of atmospheric circulation. *Geofys. Publ.*, **12,** 1–61.

Blackadar, A. K., 1979: High-resolution models of the planetary boundary layer. *Advances in Environmental Science and Engineering*, J. R. Pffafflin and E. N. Zeigler, Eds., Vol 1, No. 1, Gordon and Breach, 50–85.

Bluestein, H. B., 1993: *Synoptic-Dynamic Meteorology in Midlatitudes. Volume II: Observations and Theory of Weather Systems.* Oxford University Press, 594 pp.

Browning, K. A., and G. A. Monk, 1982: A simple model for the synoptic analysis of cold fronts. *Quart. J. Roy. Meteor. Soc.*, **108,** 435–452.

Businger, S., W. H. Bauman, and G. F. Watson, 1991: The development of the Piedmont front and associated outbreak of severe weather on 13 March 1986. *Mon. Wea. Rev.*, **119,** 2224–2251.

Carlson, T. N., 1961: Lee side frontogenesis in the Rocky Mountains. *Mon. Wea. Rev.*, **89,** 163–172.

Castle, J. A., J. D. Locatelli, J. E. Martin, and P. V. Hobbs, 1996: Structure and evolution of winter cyclones in the central United States and their effects on the distribution of precipitation. Part IV: The evolution of a drytrough on 8–9 March 1992. *Mon. Wea. Rev.*, **124,** 1591–1595.

Doswell, C. A., III, 1987: Distinction between large-scale and mesoscale contribution to severe convection: A case study example. *Wea. Forecasting,* **2,** 3–16.

Dudhia, J., 1993: A nonhydrostatic version of the Penn State–NCAR mesoscale model: Validation tests and simulation of an Atlantic cyclone and cold front. *Mon. Wea. Rev.*, **121,** 1493–1513.

Fujita, T., 1958: The structure and movement of a dry front. *Bull. Amer. Meteor. Soc.*, **39,** 574–582.

Grell, G. A., 1993: Prognostic evaluation of assumptions used by cumulus parameterizations. *Mon. Wea. Rev.*, **121,** 764–787.

——, J. Dudhia, and D. R. Stauffer, 1994: A description of the Fifth Generation Penn State/NCAR Mesoscale Model (MM5). NCAR Tech. Note NCAR/TN-398+STR, 121 pp. [Available from National Center for Atmospheric Research, Boulder, CO 80301-3000.]

Hardy, K. R., R. J. Reed, and G. K. Mather, 1973: Observations of Kelvin–Helmholtz billows and their mesoscale environment by radar, instrumented aircraft, and a dense radiosonde network. *Quart. J. Roy. Meteor. Soc.*, **99,** 279–293.

Harrold, T. W., 1973: Mechanisms influencing the distribution of precipitation within baroclinic disturbances. *Quart. J. Roy. Meteor. Soc.*, **99,** 232–251.

Hobbs, P. V., J. D. Locatelli, and J. E. Martin, 1990: Cold fronts aloft and the forecasting of precipitation and severe weather east of the Rocky Mountains. *Wea. Forecasting,* **5,** 613–626.

——, ——, and ——, 1996: A new conceptual model for cyclones generated in the lee of the Rocky Mountains. *Bull. Amer. Meteor. Soc.*, **77,** 1169–1178. (A 10-min video describing the conceptual model is available from Peter V. Hobbs, Department of Atmospheric Sciences, University of Washington, Box 351640, Seattle, WA 98195-1640.)

Holzman, B., 1936: Synoptic determination and forecasting significance of cold fronts. *Mon. Wea. Rev.*, **64,** 400–413.

Kain, J. S., and J. M. Fritsch, 1990: A one-dimensional entrainment/detrainment plume model and its application in convective parameterization. *J. Atmos. Sci.*, **47,** 2784–2802.

Lichtblau, S., 1936: Upper cold fronts in North America. *Mon. Wea. Rev.*, **64,** 414–425.

Lloyd, J. R., 1942: The development and trajectories of tornadoes. *Mon. Wea. Rev.*, **70,** 65–75.

Locatelli, J. D., and P. V. Hobbs, 1995: A world record rainfall rate at Holt, Missouri: Was it due to cold frontogenesis aloft? *Wea. Forecasting*, **10,** 779–785.

——, J. M. Sienkiewicz, and P. V. Hobbs, 1989: Organization and structure of clouds and precipitation on the mid-Atlantic coast of the United States. Part I: Synoptic evolution of a frontal system from the Rockies to the Atlantic Coast. *J. Atmos. Sci.*, **46,** 1327–1348.

——, J. E. Martin, J. A. Castle, and P. V. Hobbs, 1995: Structure and evolution of winter cyclones in the central United States and their effects on the distribution of precipitation Part III: The development of a squall line associated with weak cold-frontogenesis aloft. *Mon. Wea. Rev.*, **123,** 2641–2662.

——, M. T. Stoelinga, R. D. Schwartz, and P. V. Hobbs, 1997: Surface convergence induced by cold fronts aloft and prefrontal surges. *Mon. Wea. Rev.*, **125,** 2808–2820.

——, ——, and P. V. Hobbs, 1998: Structure and evolution of winter cyclones in the central United States and their effects on the distribution of precipitation. Part V: Thermodynamic and dual-Doppler radar analysis of a squall line associated with a cold front aloft. *Mon. Wea. Rev.*, **126,** 860–875.

——, ——, and ——, 2002: Organization and structure of clouds and precipitation on the mid-Atlantic coast of the United States. Part VII: Diagnosis of a nonconvective rainband associated with a cold front aloft. *Mon. Wea. Rev.*, **130,** 278–297.

Martin, J. E., J. D. Locatelli, and P. V. Hobbs, 1990: Organization and structure of clouds and precipitation on the mid-Atlantic coast of the United States. Part III: The evolution of a middle-tropospheric cold front. *Mon. Wea. Rev.*, **118,** 195–217.

——, ——, ——, P.-Y. Wang, and J. A. Castle, 1995: Structure and evolution of winter cyclones in the central United States and their effects on the distribution of precipitation. Part I: A synoptic-scale rainband associated with a dryline and lee trough. *Mon. Wea. Rev.*, **123,** 241–264.

McGuire, E. L., 1962: The vertical structure of three drylines as revealed by aircraft traverses. NSSP Rep. 7, 11 pp. [Available from National Severe Storms Laboratory, 1313 Halley Circle, Norman, OK 73069.]

Neiman, P. J., and R. M. Wakimoto, 1999: The interaction of a Pacific cold front with shallow masses east of the Rocky Mountains. *Mon. Wea. Rev.*, **127,** 2102–2127.

——, F. M. Ralph, M. A. Shapiro, B. F. Smull, and D. Johnson, 1998: An observational study of fronts and frontal mergers over the continental United States. *Mon. Wea. Rev.*, **126,** 2521–2554.

Reisner, J., R. T. Bruintjes, and R. M. Rasmussen, 1993: Preliminary comparisons between MM5 NCAR/Penn State model generated icing forecasts and observations. Preprints, *Fifth Int. Conf. on Aviation Weather Systems*, Vienna, VA, Amer. Meteor. Soc., 65–59.

Reitan, C. H., 1974: Frequencies of cyclones and cyclogenesis for North America, 1951–1970. *Mon. Wea. Rev.*, **102,** 861–868.

Schaefer, J. T., 1974: The life cycle of the dryline. *J. Appl. Meteor.*, **13,** 444–449.

——, 1986: The dryline. *Mesoscale Meteorology and Forecasting*, P. Ray, Ed., Amer. Meteor. Soc., 549–570.

Schultz, D. M., and W. J. Steenburgh, 1999: The formation of a forward-tilting cold front with multiple cloud bands during Superstorm 1993. *Mon. Wea. Rev.*, **127,** 1108–1124.

——, and C. A. Doswell III, 2000. Analyzing and forecasting Rocky Mountain lee cyclogenesis often associated with strong winds. *Wea. Forecasting,* **15,** 152–173.

Sienkiewicz, J. M., J. D. Locatelli, P. V. Hobbs, and B. Geerts, 1989:

Organization and structure of clouds and precipitation on the mid-Atlantic coast of the United States. Part II: The mesoscale and microscale structure of some frontal rainbands. *J. Atmos. Sci.,* **46,** 1349–1364.

Steenburgh, W. J., and C. F. Mass, 1994: The structure and evolution of a simulated Rocky Mountain lee trough. *Mon. Wea. Rev.,* **122,** 2740–2761.

Stoelinga, M. T., J. D. Locatelli, and P. V. Hobbs, 2000: Structure and evolution of winter cyclones in the central United States and their effects on the distribution of precipitation. Part VI: A multiscale numerical modeling study of the initiation of convective rainbands. *Mon. Wea. Rev.,* **128,** 3481–3500.

Wang, P.-Y., J. E. Martin, J. D. Locatelli, and P. V. Hobbs, 1995: Structure and evolution of winter cyclones in the central United States and their effects on the distribution of precipitation. Part II: Arctic fronts. *Mon. Wea. Rev.,* **123,** 1328–1344.

Williams, D. T., 1953: Pressure wave observations in the central Midwest, 1952. *Mon. Wea. Rev.,* **81,** 278–289.